

# Solid State Structures and Solution Dynamics of Unsolvated and Diethyl Ether Solvated Dilithium *N,N'*-Bis(trimethylsilyl)ethylenediamide Complexes

Michael G. Gardiner and Colin L. Raston\*

Department of Chemistry, Monash University, Clayton, Melbourne, Victoria 3168, Australia

Received August 9, 1995<sup>⊗</sup>

The lithiation of *N,N'*-bis(trimethylsilyl)ethylenediamine, **1**, by 2 equiv of methylolithium in diethyl ether yields the dimeric diethyl ether adduct [ $\{\text{Li}[\text{N}(\text{SiMe}_3)\text{CH}_2\text{CH}_2\text{NSiMe}_3\text{Li}\cdot\text{OEt}_2\}_2$ ], **2**. Recrystallization of **2** from benzene gives quantitatively the unsolvated trimer [ $\{\text{Li}[\text{N}(\text{SiMe}_3)\text{CH}_2\text{CH}_2\text{NSiMe}_3\text{Li}]\}_3$ ], **3**. The solution dynamics of **2** and **3** in toluene have been investigated using variable temperature multinuclear NMR spectroscopy. In solution, **2** is undergoing a rapid exchange process involving an equilibrium between unsolvated and diethyl ether solvated dimers, whereas compound **3** exists in a temperature dependent equilibrium of dimeric and trimeric species, of which the trimer is fluxional and exchanges inequivalent ligands by an intramolecular distortion of the  $\text{Li}_6\text{N}_6$  cage structure. Crystals of **2** are monoclinic, of space group  $P2_1/n$  (No. 14), with  $a = 10.692(9)$  Å,  $b = 16.192(2)$  Å,  $c = 24.04(4)$  Å,  $\beta = 101.16(5)^\circ$ ,  $V = 4083(8)$  Å<sup>3</sup>, and  $Z = 4$ . Crystals of **3** are trigonal, of space group  $R\bar{3}m$  (No. 166),  $a = 17.765(1)$  Å,  $c = 13.394(1)$  Å,  $V = 3660.5(5)$  Å<sup>3</sup>,  $Z = 3$ .

## Introduction

The determination of the structures of organolithium complexes in the solid state and in solution has been given much attention in recent years.<sup>1,2</sup> Characterization has relied heavily on X-ray crystal structure determination and multinuclear NMR spectroscopy and cryoscopy measurements to determine the extent of aggregation of the complexes in solution. From this, and associated theoretical molecular orbital calculations, has developed an understanding of the association of such species and dynamic processes which explain exchange and fluxional processes in solvated and unsolvated complexes. Herein we report the syntheses, X-ray crystal structures, and solution dynamics of two dilithiated *N,N'*-bis(trimethylsilyl)ethylenediamine complexes as an extension of our studies of polyolithiated secondary amines.<sup>3</sup> We find that in the solid state diethyl ether complexation is effective in reducing the aggregation of the complex to a dimer from the trimeric form established for the unsolvated compound. In toluene solution, the diethyl ether solvated dimeric complex is undergoing a decomplexation/complexation process and the unsolvated complex is present as a slowly exchanging equilibrium of dimeric and trimeric forms, the trimer undergoing an intramolecular fluxional process involving a distortion of the  $\text{Li}_6\text{N}_6$  cage.

## Experimental Section

**Syntheses.** All manipulations were carried out using standard Schlenk and glovebox techniques under an atmosphere of high purity argon or nitrogen. Solvents were dried then freeze/thaw degassed prior to use. *N,N'*-Bis(trimethylsilyl)ethylenediamine was prepared according to an adapted literature procedure.<sup>4</sup> *n*-BuLi was obtained from Metallgesellschaft (AG) as a 1.60 M solution in hexane and was standardized prior to use. All other reagents were obtained from Aldrich. <sup>1</sup>H NMR spectra were recorded on Bruker WM-250, CXP-300, and Varian

Gemini-200 and Unity-400 spectrometers in deuterated benzene and toluene and referenced to the residual <sup>1</sup>H resonances of the solvent ( $\delta$  7.15 and 6.98, respectively). <sup>7</sup>Li NMR spectra were recorded on Bruker CXP-300 and Varian Unity-400 spectrometers operating at 116.6 and 155.5 MHz, respectively, in deuterated benzene or toluene and referenced to external  $\text{LiNO}_3$  (1 M in  $\text{D}_2\text{O}$ ,  $\delta$  0.00). <sup>13</sup>C NMR spectra were recorded in deuterated benzene on Bruker WM-250 and Varian Gemini-200 spectrometers operating at 62.8 and 50.3 MHz, respectively, using broad band proton decoupling and were referenced to the <sup>13</sup>C resonances of the deuterated solvents ( $\delta$  128.0). Elemental analyses were performed by the Canadian Microanalytical Services Ltd., Vancouver, BC, and the Chemical and Micro-Analytical Services Pty. Ltd., Melbourne, Australia. Melting points were determined in sealed glass capillaries under argon and are uncorrected. IR spectra were recorded as Nujol mulls on NaCl plates using a Perkin-Elmer 1725X Fourier transformed infrared spectrometer.

**Synthesis of [ $\{\text{Li}[\text{N}(\text{SiMe}_3)\text{CH}_2\text{CH}_2\text{NSiMe}_3\text{Li}\cdot\text{OEt}_2\}_2$ ], **2**.** To a stirred solution of *N,N'*-bis(trimethylsilyl)ethylenediamine, **1** (1.94 g, 8.96 mmol), in diethyl ether (30 mL) was added MeLi (12.8 mL, 1.4 M in diethyl ether, 17.92 mmol) over 10 min at 0 °C. The colorless solution was allowed to warm to room temperature and was stirred for 1 h. The solution was concentrated *in vacuo* and cooled to  $-30$  °C, whereupon large colorless crystals of the *title compound* deposited overnight. Subsequent cropping of the crystals yielded further product (2.43 g, 88% yield). Mp: 77 °C dec. <sup>1</sup>H NMR (250 MHz,  $\text{C}_6\text{D}_6$ ):  $\delta$  0.22 (36 H, s,  $\text{SiMe}_3$ ), 1.01 (12 H, t <sup>3</sup> $J_{\text{H-H}} = 7.03$  Hz, Me), 3.18 (8 H, s, N-CH<sub>2</sub>), 2.25 (8 H, q <sup>3</sup> $J_{\text{H-H}} = 7.03$  Hz, O-CH<sub>2</sub>). <sup>13</sup>C NMR (62.8 MHz,  $\text{C}_6\text{D}_6$ ):  $\delta$  1.1 ( $\text{SiMe}_3$ ), 14.8 (Me), 52.4 (N-CH<sub>2</sub>), 65.4 (O-CH<sub>2</sub>). <sup>7</sup>Li NMR (116.6 MHz,  $\text{C}_6\text{D}_6$ ):  $\delta$   $-0.62$ . Anal. Calcd: C, 49.62; H, 11.10; N, 9.64. Found: C, 49.02; H, 10.66; N, 9.73.

**Synthesis of [ $\{\text{Li}[\text{N}(\text{SiMe}_3)\text{CH}_2\text{CH}_2\text{NSiMe}_3\text{Li}]\}_3$ ], **3**.** Compound **2** (1.00 g, 4.62 mmol) was dissolved in benzene (10 mL) and the solution stirred for 1 h. The volatiles were removed *in vacuo* to yield an analytically pure sample of the *title compound* (0.72 g, 97% yield). The compound was crystallized with difficulty in low yield from a minimal amount of the same solvent. Mp: 115–118 °C. <sup>1</sup>H NMR (200 MHz,  $\text{C}_6\text{D}_6$ ):  $\delta$

<sup>⊗</sup> Abstract published in *Advance ACS Abstracts*, June 1, 1996.

- (1) Gregory, K.; Schleyer, P. v. R.; Snaith, R. *Adv. Inorg. Chem.* **1991**, *37*, 47.
- (2) Mulvey, R. E. *Chem. Soc. Rev.* **1991**, *20*, 167.
- (3) Gardiner, M. G.; Raston, C. L. *Inorg. Chem.* **1995**, *34*, 4206.
- (4) West, R.; Ishikawa, M.; Murai, S. *J. Am. Chem. Soc.* **1968**, *90*, 727.

**Table 1.** Crystal Data for  $[\{\text{Li}[\text{N}(\text{SiMe}_3)\text{CH}_2\text{CH}_2\text{NSiMe}_3]\text{Li}\cdot\text{OEt}_2\}_2]$ , **2**, and  $[\{\text{Li}[\text{N}(\text{SiMe}_3)\text{CH}_2\text{CH}_2\text{NSiMe}_3]\text{Li}\}_3]$ , **3**

<b>2:</b> $\text{C}_{24}\text{H}_{64}\text{N}_4\text{Li}_4\text{O}_2\text{Si}_4$	fw = 580.90
$a = 10.692(9)$ Å	space group: $P2_1/n$ (No. 14)
$b = 16.192(2)$ Å	$T = 24^\circ\text{C}$
$c = 24.04(4)$ Å	$\lambda = 0.710\ 69$ Å
$\beta = 101.16(5)^\circ$	$\rho_{\text{calcd}} = 0.945$ g cm $^{-3}$
$V = 4083(8)$ Å $^3$	$\mu = 1.67$ cm $^{-1}$
$Z = 4$	$R^a = 0.059$
	$R_w^b = 0.073$ (unit weights)
<b>3:</b> $\text{C}_{24}\text{H}_{66}\text{N}_6\text{Li}_6\text{Si}_6\cdot\text{C}_6\text{H}_6$	fw = 648.99
$a = 17.765(1)$ Å	space group: $R\bar{3}m$ (No. 166)
$c = 13.394(1)$ Å	$T = 24^\circ\text{C}$
$V = 3660.5(5)$ Å $^3$	$\lambda = 0.710\ 69$ Å
$Z = 3$	$\rho_{\text{calcd}} = 0.999$ g cm $^{-3}$
	$\mu = 1.96$ cm $^{-1}$
	$R^a = 0.121$
	$R_w^b = 0.106$ (unit weights)

$$^a R = \sum ||F_o| - |F_c|| / \sum |F_o|, \quad ^b (R_w = (\sum w||F_o| - |F_c||^2 / \sum w|F_o|^2)^{1/2}).$$

0.11, 0.18 ( $2 \times 18$  H (*ca.* 2:1), s, SiMe $_3$ ), 3.08 ( $2 \times 4$  H, s, N-CH $_2$ ).  $^{13}\text{C}$  NMR (50 MHz, C $_6\text{D}_6$ ):  $\delta$  0.2, 1.3 (SiMe $_3$  (*ca.* 2:1)), 50.3, 51.7 (N-CH $_2$  (*ca.* 2:1)).  $^7\text{Li}$  NMR (155.5 MHz, C $_6\text{D}_6$ ):  $\delta$  1.22, 1.39 (*ca.* 2:1). Anal. Calcd: C, 44.42; H, 10.25; N, 12.8. Found: C, 44.44; H, 10.38; N, 12.88.

**Structure Determinations.** Crystals of **2** and **3** suitable for X-ray structure determination were grown from diethyl ether and benzene solutions at  $-30^\circ\text{C}$  and were mounted in sealed capillaries under an argon atmosphere. Unique diffractometer data sets were measured on colorless crystals using an Enraf-Nonius CAD4 diffractometer with a graphite single-crystal monochromator ( $2\theta_{\text{max}} = 50^\circ$ ). Reflections with  $I > 2.5\sigma(I)$  were considered "observed" and used in the full-matrix least-squares refinements, minimizing  $\sum w\Delta^2$  after solution of the structures by direct methods. Conventional residuals on  $F$  at convergence are quoted. No extensive, significant extinction effects were found. Neutral-atom complex scattering factors were employed.<sup>5</sup> Computation used the XTAL 3.0<sup>6</sup> program system implemented on a Sun SPARCstation 2 computer. Molecular core geometries, atom coordinates, and crystal data are given in Tables 1–5, and molecular projections showing numbering schemes are given in Figures 3 and 4. Averaged structural parameters will be used in the structural comparisons where appropriate, and are distinguished by the absence of the least-squares error term from the determined quantity. Anisotropic thermal parameters were refined for all non-hydrogen atoms in **2** and most non-hydrogen atoms in **3** (except N(2) and C(2)). Methyl and methylene hydrogen atoms were calculated and constrained at estimated values (C–H 1.0 Å). Temperature factors for methyl hydrogen atoms were estimated at  $1.5U_{ii}$  (average) of the attached carbon atom and  $1.25U_{ii}$  (average) for methylene hydrogen atoms. A packing disorder of the diethyl ether molecules of **2** was apparent in Fourier maps which could not be successfully modelled. Severe disorder was present in the structure of **3**, which is described in the X-ray structure commentary section. Refinement was by a single conformation with large anisotropic thermal parameters. Hydrogen atoms were not included for the disordered diethyl ether molecules of **2**, the methylene groups of **3**, and the benzene molecule of crystallization in **3**.

**Table 2.** Non-Hydrogen Atom Coordinates and Isotropic Thermal Parameters for  $[\{\text{Li}[\text{N}(\text{SiMe}_3)\text{CH}_2\text{CH}_2\text{NSiMe}_3]\text{Li}\cdot\text{OEt}_2\}_2]$ , **2**

atom	$x/a$	$y/b$	$z/c$	$U, \text{Å}^2$
Li1	0.099(2)	0.333(1)	0.2708(7)	0.087(7)
Li2	0.193(1)	0.406(1)	0.3552(7)	0.073(6)
Li3	0.284(1)	0.292(1)	0.4054(6)	0.073(6)
Li4	0.094(2)	0.245(1)	0.4349(7)	0.079(7)
N1	0.2838(6)	0.3135(4)	0.3220(3)	0.065(3)
N4	0.2204(7)	0.1818(4)	0.4032(3)	0.067(3)
N5	0.1546(6)	0.3698(4)	0.4323(3)	0.064(3)
N8	0.0178(6)	0.4157(4)	0.3128(3)	0.072(3)
Si1	0.4119(3)	0.3646(2)	0.3059(1)	0.086(1)
C2	0.2852(9)	0.2236(6)	0.3114(4)	0.075(4)
C3	0.1949(9)	0.1758(6)	0.3412(4)	0.080(4)
Si4	0.3050(3)	0.1069(2)	0.4422(1)	0.079(1)
Si5	0.2473(3)	0.4136(2)	0.4905(1)	0.085(1)
C6	0.0228(9)	0.4041(6)	0.4177(4)	0.080(4)
C7	-0.0434(8)	0.3831(6)	0.3582(4)	0.081(4)
Si8	-0.0356(3)	0.5036(2)	0.2795(1)	0.088(1)
C11	0.570(1)	0.3240(9)	0.3453(6)	0.139(7)
C12	0.423(1)	0.3648(8)	0.2289(5)	0.129(6)
C13	0.398(1)	0.4747(7)	0.3282(6)	0.130(7)
C41	0.484(1)	0.1121(8)	0.4453(5)	0.120(6)
C42	0.257(1)	-0.0010(7)	0.4183(5)	0.126(6)
C43	0.283(1)	0.1189(8)	0.5175(4)	0.117(6)
C51	0.4117(9)	0.3678(8)	0.4960(5)	0.121(6)
C52	0.198(1)	0.3923(8)	0.5602(4)	0.127(6)
C53	0.259(1)	0.5299(7)	0.4861(6)	0.141(7)
C81	0.025(1)	0.5068(8)	0.2110(5)	0.145(7)
C82	0.024(1)	0.6022(7)	0.3186(5)	0.129(6)
C83	-0.215(1)	0.5141(8)	0.2630(5)	0.143(7)
O1	0.0063(9)	0.2730(6)	0.2053(3)	0.131(4)
O4	-0.0551(8)	0.1988(6)	0.4589(4)	0.128(4)
C1o	0.050(4)	0.229(2)	0.156(1)	0.28(3)
C2o	0.114(3)	0.269(2)	0.136(1)	0.26(2)
C3o	-0.124(2)	0.250(2)	0.209(2)	0.32(2)
C4o	-0.210(2)	0.268(2)	0.204(1)	0.27(2)
C5o	-0.115(3)	0.128(2)	0.437(1)	0.29(2)
C6o	-0.135(3)	0.108(2)	0.3905(8)	0.27(2)
C7o	-0.108(3)	0.235(2)	0.506(1)	0.30(2)
C8o	-0.079(3)	0.215(2)	0.552(1)	0.30(2)

<sup>a</sup> Isotropic equivalent thermal parameters.

**Table 3.** Non-Hydrogen Atom Coordinates and Isotropic Thermal Parameters for  $[\{\text{Li}[\text{N}(\text{SiMe}_3)\text{CH}_2\text{CH}_2\text{NSiMe}_3]\text{Li}\}_3]$ , **3**

atom	$x/a$	$y/b$	$z/c$	$U, \text{Å}^2$	population
Li	0.724(1)	$2X - 1$	0.777(2)	0.14(2) <sup>aa</sup>	
N1	0.6110(8)	$-X + 1$	0.720(2)	0.10(1) <sup>a</sup>	0.6667
C1	0.636(1)	$-X + 1$	0.629(2)	0.24(3) <sup>a</sup>	0.6667
Si	0.5564(2)	$-X + 1$	0.6867(5)	0.163(5) <sup>a</sup>	
C11	0.463(1)	0.378(2)	0.615(2)	0.45(2) <sup>a</sup>	
C12	0.526(1)	$-X + 1$	0.817(3)	0.45(5) <sup>a</sup>	
N2	0.743(1)	$2X - 1$	0.912(4)	0.08(2)	0.3333
C2	0.714(4)	0.551(4)	0.851(5)	0.13(3)	0.1667
C1s	0.706(1)	$2X - 1$	0.354(2)	0.42(4) <sup>a</sup>	

<sup>a</sup> Isotropic equivalent thermal parameters.

## Discussion

**Synthesis.** The lithiation of *N,N'*-bis(trimethylsilyl)ethylenediamine, **1**, by 2 equiv of MeLi in diethyl ether yielded the dimeric diethyl ether solvated adduct of the substituted *N,N'*-dilithiated ethylenediamine  $[\{\text{Li}[\text{N}(\text{SiMe}_3)\text{CH}_2\text{CH}_2\text{NSiMe}_3]\text{Li}\cdot\text{OEt}_2\}_2]$ , **2**. Recrystallization of **2** from benzene or toluene gave quantitatively the unsolvated compound  $[\{\text{Li}[\text{N}(\text{SiMe}_3)\text{CH}_2\text{CH}_2\text{NSiMe}_3]\text{Li}\}_3]$ , **3**, as did lithiation of **1**, by 2 equiv of *n*-BuLi in hexane. Both complexes could be isolated in high yield as very air and moisture sensitive, colorless crystalline solids from the respective synthetic route, Scheme 1.

The dilithiations of **1** by alkyl lithium species outlined in Scheme 1 differ from the analogous lithiations of *N,N'*-di-*tert*-butylethylenediamine<sup>7</sup> in three respects. Dilithiation of the

(5) *International Tables for X-ray Crystallography*; Ibers, J. A., Hamilton, W. C., Eds.; Kynoch Press: Birmingham, England, 1974; Vol. 4.  
 (6) *XTAL User's Manual—Version 3.0*; Hall, S. R., Stewart, J. M., Eds.; The Universities of Western Australia and Maryland; Nedland, Australia, and College Park, MD, 1990.

**Table 4.** Selected Structural Parameters for  $[\{\text{Li}[\text{N}(\text{SiMe}_3)\text{CH}_2\text{CH}_2\text{NSiMe}_3\text{Li}\cdot\text{OEt}_2\}_2]$ , **2**

Bond Distances (Å)					
Li1-N1	2.14(2)	Li4-N5	2.12(2)	Si5-N5	1.704(7)
Li1-N8	1.98(2)	Li4-O4	1.95(2)	Si8-N8	1.678(7)
Li1-O1	1.95(2)	N1-C2	1.48(1)	O1-C1o	1.53(3)
Li2-N1	2.04(2)	C2-C3	1.52(1)	O1-C3o	1.46(3)
Li2-N5	2.06(2)	N4-C3	1.47(1)	O4-C5o	1.36(3)
Li2-N8	1.95(1)	N5-C6	1.49(1)	O4-C7o	1.48(4)
Li3-N1	2.03(2)	C6-C7	1.51(1)	C5o-C6o	1.15(4)
Li3-N4	1.91(2)	N8-C7	1.47(1)	C7o-C8o	1.14(4)
Li3-N5	2.06(2)	Si1-N1	1.709(8)	C2o-C1o	1.12(5)
Li4-N4	1.96(2)	Si4-N4	1.685(7)	C4o-C3o	0.95(3)
Contact Distances (Å)					
Li1-Li2	2.40(2)	Li3-Li4	2.40(2)	N8-Li1	4.02
Li2-Li3	2.31(2)	N4-Li4	4.00		
Bond Angles (deg)					
N1-Li1-N8	104.6(8)	Li4-N4-Si4	119.7(6)		
N1-Li1-O1	132(1)	Li4-N4-C3	115.0(7)		
N8-Li1-O1	123.1(9)	Si4-N4-C3	119.5(6)		
N1-Li2-N5	109.5(8)	Li2-N5-Li3	68.3(6)		
N1-Li2-N8	109.7(7)	Li2-N5-Li4	114.3(7)		
N5-Li2-N8	99.1(7)	Li2-N5-Si5	115.8(6)		
N1-Li3-N4	101.3(7)	Li2-N5-C6	91.3(6)		
N1-Li3-N5	109.6(7)	Li3-N5-Li4	69.9(7)		
N4-Li3-N5	108.8(8)	Li3-N5-Si5	101.0(5)		
N4-Li4-N5	104.5(8)	Li3-N5-C6	144.4(7)		
N4-Li4-O4	125.4(9)	Li4-N5-Si5	120.2(5)		
N5-Li4-O4	130.0(9)	Li4-N5-C6	94.8(7)		
Li1-N1-Li2	70.1(6)	Si5-N5-C6	114.3(6)		
Li1-N1-Li3	114.6(7)	N5-C6-C7	112.8(8)		
Li1-N1-Si1	119.5(6)	N8-C7-C6	115.3(7)		
Li1-N1-C2	94.7(7)	Li1-N8-Li2	75.2(7)		
Li2-N1-Li3	69.3(7)	Li1-N8-Si8	118.4(7)		
Li2-N1-Si1	101.4(6)	Li1-N8-C7	115.7(8)		
Li2-N1-C2	144.7(7)	Li2-N8-Si8	121.2(6)		
Li3-N1-Si1	117.2(5)	Li2-N8-C7	95.8(7)		
Li3-N1-C2	90.5(7)	Si8-N8-C7	119.9(6)		
Si1-N1-C2	113.7(6)	Li1-O1-C1o	132(2)		
N1-C2-C3	112.9(8)	Li1-O1-C3o	115(2)		
N4-C3-C2	115.8(7)	C1o-O1-C3o	111(2)		
Li3-N4-Li4	76.5(7)	Li4-O4-C5o	124(2)		
Li3-N4-Si4	120.6(6)	Li4-O4-C7o	122(1)		
Li3-N4-C3	94.9(7)	C5o-O4-C7o	114(2)		

ethylenediamine in this case is rapid and the monolithiated complex is not isolable; lithiations of **1** with 1 equiv of MeLi in diethyl ether gives a mixture of unreacted **1** and the dilithiated product, **2**. In addition, the completely lithiated product can be isolated as crystalline solvent free and diethyl ether adducts, contrasting with microcrystalline powders for the *t*-Bu analogue when recrystallized from hydrocarbon solvents and diethyl ether by slow cooling of saturated solutions.

The lithium compounds were characterized by X-ray crystal structure determination,  $^1\text{H}$ ,  $^7\text{Li}$ , and  $^{13}\text{C}$  NMR, and IR spectroscopy and gave satisfactory microanalyses.

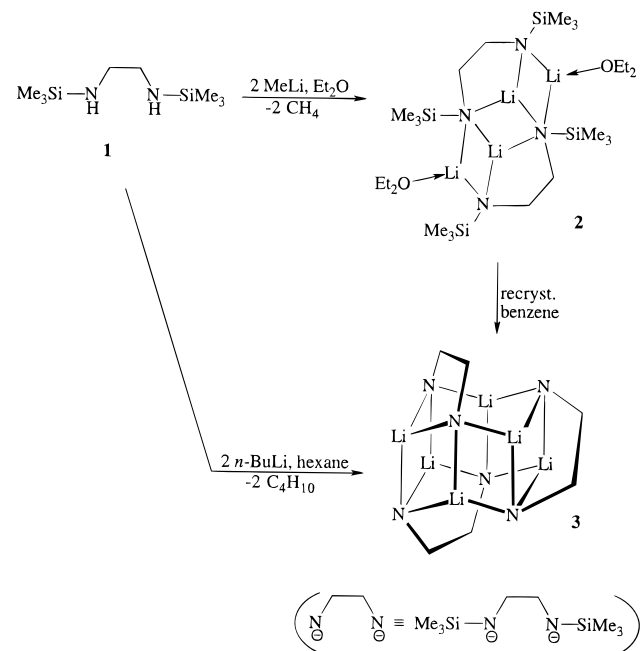
**NMR Spectroscopy.** The X-ray crystal structure of **2**, *vide infra*, shows the molecule to be dimeric in the solid state. The complex is best described as a diethyl ether complexed amidolithium dimer containing a four-rung  $\text{Li}_4\text{N}_4$  ladder core with the ethylene linkages of the dilithiated ethylenediamines "edge-bridging" nitrogen atoms along the ladder, pulling the ladder into a "concave" shape.

In solution **2** is undergoing a rapid exchange process. The room temperature  $^7\text{Li}$  NMR spectrum, Figure 1, shows the presence of a single resonance at  $-0.62$  ppm. Cooling the sample results in the resonance broadening and eventually splitting at *ca.*  $-35$  °C. Further cooling gives two resonances at  $+1.12$  and  $-1.05$  ppm of near equal intensity, which is

**Table 5.** Selected Structural Parameters for  $[\{\text{Li}[\text{N}(\text{SiMe}_3)\text{CH}_2\text{CH}_2\text{NSiMe}_3\text{Li}\}_3]$ , **3**

Bond Distances (Å)					
Li-N1'	1.90(2)	N1-Si	1.74(2)	C2-C2''*	1.52(9)
Li''*-N1'	2.27(4)	N1-C1	1.44(3)	Si-N2	1.38(6)
Li-N2''*	1.90(6)	C1'-C1''	1.65(4)		
Li-N2	2.15(4)	N2-C2	1.7(1)		
Contact Distances (Å)					
Li-Li''*	2.32(4)	N1'-N1''	2.96(3)	N1'-N2''*	3.32(5)
Li-Li''	3.06(4)	N1'-N1*	3.48(3)	N2-N2''*	3.16(5)
N1'-Li''	3.56(4)	N1'-N2	3.57(6)		
Bond Angles (degrees)					
N1'-Li'-N1''	103(2)	N1'-C1'-C1''	117(2)		
N1'-Li'-N1*	113(1)	C12-Si-N2	77(3)		
N1'-Li-N2''*	122(2)	C11-Si-N2	123(2)		
N1'-Li-N2	124(2)	Li''*-N2-C2	74(3)		
N2-Li-N2''*	103(2)	C2-N2-Li''	143(4)		
C1'-N1'-Si'	107(1)	C2-N2-Li	83(3)		
C1'-N1'-Li	96(2)	C2-N2-Si	83(3)		
C1'-N1'-Li''*	150(2)	Li-N2-Li''	91(2)		
Si'-N1'-Li	122(1)	Li-N2-Li''*	70(2)		
Si'-N1'-Li''*	103(1)	Li-N2-Si	127(3)		
Li-N1'-Li'	67(2)	Li''*-N2-Si	150(3)		
Li-N1'-Li''*	107(2)	N2-C2-C2''*	114(7)		

\* Key: single and double primes denote  $C_3$  symmetry operators; an asterisk denotes a  $C_2$  symmetry operator; a plus sign denotes a  $C_s$  symmetry operator.

**Scheme 1**

consistent with the solid state structure of the dimeric tetranuclear etherate complex of  $C_2$  symmetry.

The  $^1\text{H}$  NMR spectrum of **2**, Figure 1, exhibits a temperature dependence similar to that observed in the  $^7\text{Li}$  NMR spectrum which is also consistent with the crystal structure of the complex at low temperature. At room temperature, single resonances are observed for the trimethylsilyl group protons and the methylene protons of the dilithiated ethylenediamine in addition to resonances for the diethyl ether molecules. When the sample is cooled, the proton resonance for the trimethylsilyl group shifts substantially between room temperature and  $-40$  °C and at *ca.*  $-65$  °C splits to give two resonances of equal intensity. Similarly, the methylene resonance broadens and splits into multiple resonances showing multiplet structure at close to the same temperature. Significant shifts and line broadening is also observed for the diethyl ether resonances over this temperature

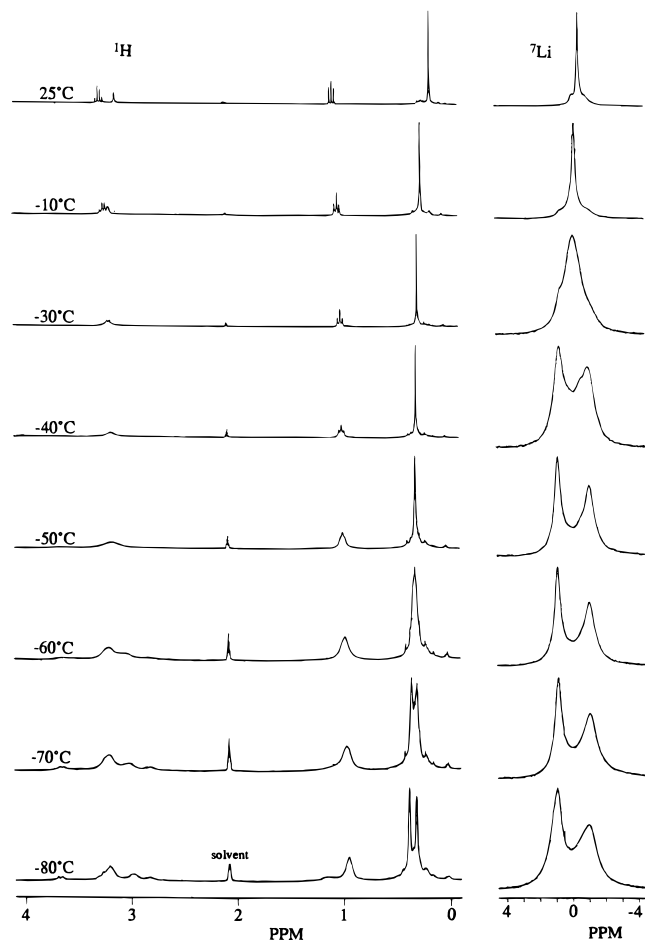


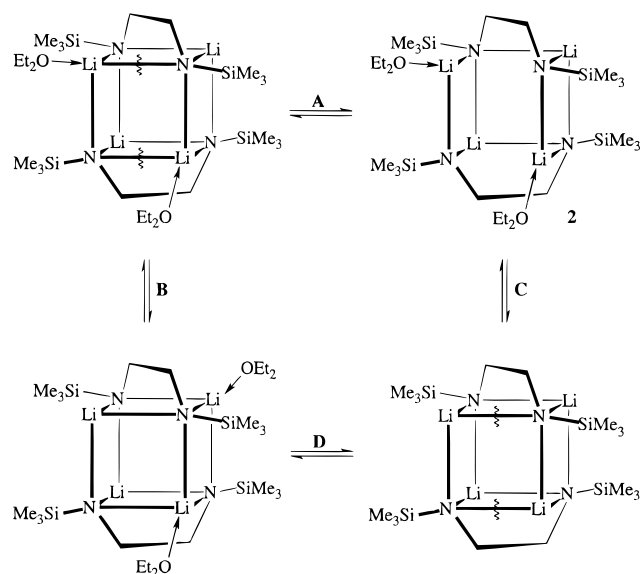
**Figure 1.** Variable temperature  $^1\text{H}$  and  $^7\text{Li}$  NMR spectra of  $[\{\text{Li}[\text{N}(\text{SiMe}_3)\text{CH}_2\text{CH}_2\text{NSiMe}_3]\text{Li}\cdot\text{OEt}_2\}_2]$ , **2**, in toluene- $d_8$ , at 300 and 116.6 MHz, respectively.

range. The  $^{13}\text{C}$  NMR spectrum of **2** also shows the presence of a ligand with equivalent trimethylsilyl and methylene carbon atoms at room temperature. The temperature dependence of the  $^{13}\text{C}$  NMR spectrum was not investigated.

The process which gives rise to the room temperature equivalence of both ends of the ethylenediamido ligand most likely arises from exchange processes involving the diethyl ether molecules, as shown in Scheme 2; the structure in the upper right depicts the crystal structure of **2**. The structure can be seen to resemble a stacked dimer of  $[\{\text{Li}[\text{N}(\text{SiMe}_3)\text{CH}_2\text{CH}_2\text{NSiMe}_3]\text{Li}\}_2]$  which has been capped on two corners of the  $\text{Li}_4\text{N}_4$  cage by two molecules of diethyl ether, resulting in cleavage of two edges of the cage to give the observed four-rung  $\text{Li}_4\text{N}_4$  ladder structure, equilibrium **A**. This is likely to be a low energy process given that the formation of the two  $\text{Li}-\text{O}$  bonds is at the expense of two  $\text{Li}-\text{N}$  bonds. The specific equilibrium responsible for the simplification of the  $^1\text{H}$  NMR spectrum of **2** at room temperature is conceivably the migration of the diethyl ether molecules from corner-to-corner of the solvated cage, equilibrium **B**, or the reversible complexation/decomplexation of the diethyl ether molecules associated with the cage structure, equilibria **C** and **D**. Of these processes, the latter are favored given that **2** recrystallizes from benzene and toluene solutions as a trimer devoid of diethyl ether.

The dimeric stack proposed for the solution structure of **2** relates to the well-established formation of tetrameric and hexameric aggregates of simple alkyl lithium species. For instance, methyl lithium exists as a tetramer containing a  $\text{Li}_4\text{C}_4$  cage in the solid state<sup>8</sup> and in solution.<sup>9</sup> In the solid state the tetrameric units of methyl lithium also exhibit weak  $\text{Li}-\text{H}$

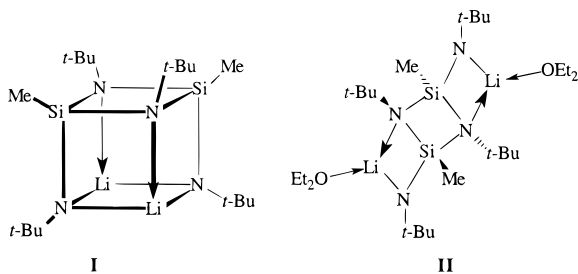
## Scheme 2



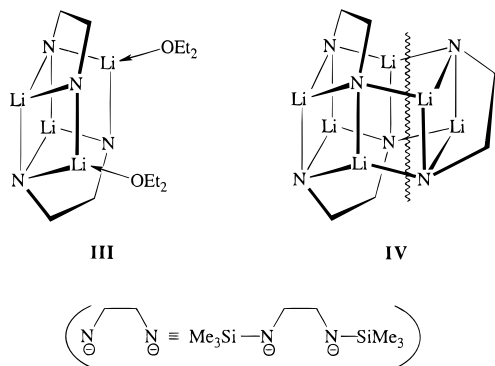
contacts to the methyl protons of adjacent aggregates forming an extended network structure which accounts for its limited solubility in noncoordinating solvents and low volatility. In coordinating solvents (diethyl ether and tetrahydrofuran), the tetrameric unit is retained and the  $\text{Li}-\text{H}$  contacts of the solid state structure are replaced with coordination by the Lewis base donor molecules to the Li vertices of the aggregate. This structural type has been authenticated in one case,<sup>10</sup>  $\{(\text{MeLi})_4-(N,N,N',N'-\text{tetramethylethylenediamine})_2\}_n$ . For steric reasons, the common structural  $\text{Li}_6\text{N}_6$  cage motif of imidolithium chemistry can only be capped on the lithium vertices (with retention of cage structures) when aryl C-substituents are present and then with a concomitant decrease in the size of the aggregate to a  $\text{Li}_4\text{N}_4$  cage. The crystal structures of  $[\{\text{LiN}=\text{C}(\text{Ph})(t\text{-Bu})\}_6]$ <sup>11</sup> and  $[\{\text{C}_5\text{H}_5\text{N}\cdot\text{LiN}=\text{CPh}_2\}_4]$ <sup>12</sup> stand as pertinent examples. In the case of **2**, the steric hindrance afforded to the open coordination face of the naked lithium vertices of the  $\text{Li}_4\text{N}_4$  cage by the trimethylsilyl substituents is intramolecular and protects the lithium atoms in solution. Because of this, any solvation of **2** must be at the expense of the integrity of the  $\text{Li}_4\text{N}_4$  cage, giving the observed  $\text{Li}_4\text{N}_4$  ladder structure. In a similar manner, the monomeric *cis*- and *trans*-isomers of the dilithio-derivatives  $[\text{cis}\{-\{(t\text{-Bu})\text{NSi}(\text{Me})\text{N}(t\text{-Bu})\text{Li}\}_2\}]$ , **I**, and  $[\text{trans}\{-\{(t\text{-Bu})\text{NSi}(\text{Me})\text{N}(t\text{-Bu})\text{Li}\cdot\text{OEt}_2\}_2\}]$ , **II**, exhibit unsolvated  $\text{Li}_2\text{N}_4\text{Si}_2$  cage and bis(diethyl ether) solvated  $\text{Li}_2\text{N}_4\text{Si}_2$  ladder structures.<sup>13</sup>

The X-ray crystal structure of the solvent free complex **3**, *vide infra*, shows the molecule to be trimeric in the solid state. The complex contains a cyclic six-rung  $\text{Li}_6\text{N}_6$  ladder core with two of the three ethylene linkages of the dilithiated ethylenediamines “edge-bridging” nitrogen atoms on either side of the ladder while the third ethylene linkage “face-bridges” nitrogen atoms of adjacent ladder rungs.

- (8) (a) Weiss, E.; Lucken, E. A. C. *J. Organomet. Chem.* **1964**, *2*, 197. (b) Weiss, E.; Hencken, G. *J. Organomet. Chem.* **1970**, *21*, 265. (c) Weiss, E.; Lambertsen, T.; Schubert, B.; Cockcroft, J. K.; Wiedenmann, A. *Chem. Ber.* **1990**, *123*, 79.
- (9) Wakefield, B. J. *The Chemistry of Organolithium Compounds*; Pergamon: Oxford, England, 1974.
- (10) Köster, H.; Thoennes D.; Weiss, E. *J. Organomet. Chem.* **1978**, *160*, 1.
- (11) Barr, D.; Clegg, W.; Mulvey, R. E.; Snaith, R.; Wade, K. *J. Chem. Soc., Chem. Commun.* **1986**, 295.
- (12) Barr, D.; Clegg, W.; Mulvey, R. E.; Snaith, R. *J. Chem. Soc., Chem. Commun.* **1984**, 79.
- (13) Veith, M.; Goffing, F.; Huch, V. *Chem. Ber.* **1988**, *121*, 943.



In the solid state, compound **3** maintains the same  $\text{Li}_4\text{N}_4$  ladder core of the etherate **2**, albeit having the coordinated ether molecules removed from the terminal lithium atoms. The effect of this structural motif on **3**, as it was in **2**, is to pull the ladder into a "concave" or "U-shape" such that the terminal nitrogen and lithium atoms can be spanned by an additional bridging monomeric unit of the complex to give the observed cyclic six-rung  $\text{Li}_6\text{N}_6$  ladder core, as depicted in **III** and **IV**, which depict the complexes **2** and **3**, respectively. Figures 3 and 4 show molecular projections of the crystal structures of both the dimeric etherate **2** and unsolvated trimer **3** which illustrate that the relative stereochemistry of the ligands in the etherate is unchanged in the unsolvated complex.



The  $^1\text{H}$  and  $^7\text{Li}$  NMR spectra of the unsolvated complex **3** do not exhibit the same temperature dependence as those of the etherate **2**. Moreover, at room temperature the complex exists as an equilibrium of two species in a *ca.* 2:1 ratio, assigned as the dimeric and trimeric species, respectively. The assignment of dimeric and trimeric forms in benzene and toluene solutions is based on the concentration and temperature dependence of the  $^1\text{H}$  and  $^7\text{Li}$  NMR spectra.

Variable temperature  $^1\text{H}$  and  $^7\text{Li}$  NMR studies of **3** show that the species distribution is temperature dependent and also reveals a fluxional process for one of the species, Figure 2. At  $50^\circ\text{C}$ , the major species in solution, *ca.* 90%, exhibits single sharp resonances for both the protons of the trimethylsilyl groups and the methylene protons of the dilithiated ethylenediamine at 0.07 and 3.08 ppm, respectively. At lower temperatures, the species distribution reverses, such that below  $-20^\circ\text{C}$  the aforementioned species is present in only *ca.* 20%. Lowering the temperature further has little effect on the species distribution and has little effect on the appearance of the resonances associated with the aforementioned species. Upon dilution of the NMR sample, the room temperature species distribution becomes further skewed in favor of the same species which is consistent with the level of aggregation of this species being the lower of the two.

The minor species in solution at *ca.*  $5^\circ\text{C}$  and above exhibits a single sharp resonance for the trimethylsilyl group protons at 0.14 ppm and two distinguishable methylene proton resonances having multiplet structure between 2.9–3.3 ppm. Below this

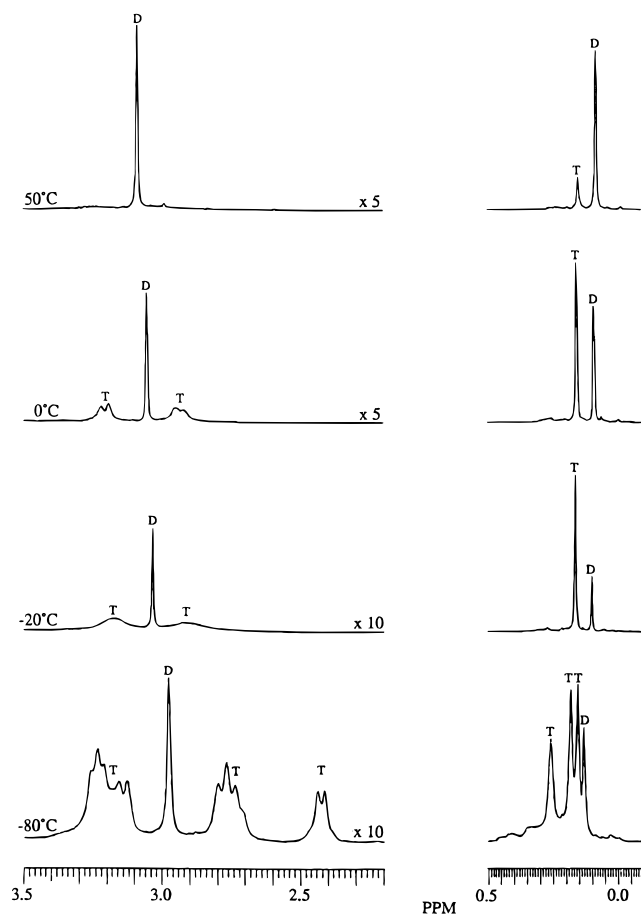


**Figure 2.** Variable temperature  $^1\text{H}$  NMR spectra of  $[\{\text{Li}[\text{N}(\text{SiMe}_3)\text{CH}_2\text{CH}_2\text{NSiMe}_3]\text{Li}\}_3]$ , **3**, in toluene- $d_8$ , at 400 MHz. Resonances for the dimer are labeled "D" and for the trimer are labeled "T".

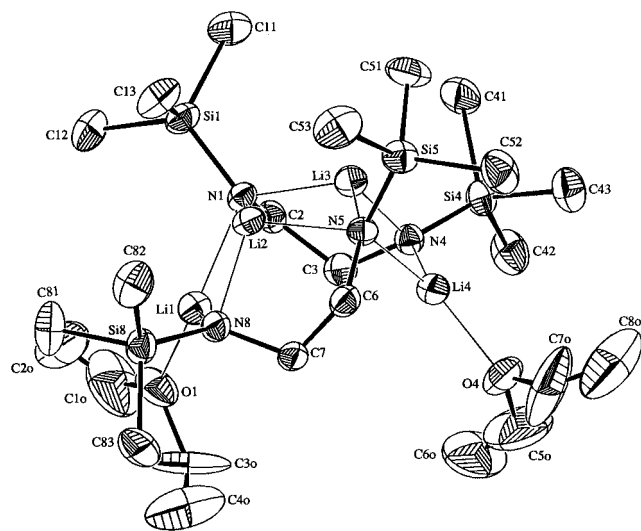


**Figure 3.** Molecular projection of  $[\{\text{Li}[\text{N}(\text{SiMe}_3)\text{CH}_2\text{CH}_2\text{NSiMe}_3]\text{Li}\cdot\text{OEt}_2\}_2]$ , **2**, showing the atom-labeling scheme. Thermal ellipsoids are drawn at the 20% probability level.

temperature, the species distribution favors this species and at *ca.*  $-20^\circ\text{C}$  the resonances of these methylene protons broaden and then split to give six identifiable signals. Similarly, at  $-50^\circ\text{C}$  the resonance of the trimethylsilyl group protons associated with the methylene protons splits to give three signals of equal intensity.

The room temperature  $^7\text{Li}$  NMR spectrum of **3** consists of two broad signals at 1.30 and 1.12 ppm in a *ca.* 1:2 ratio which are further skewed at higher temperatures and show no signs

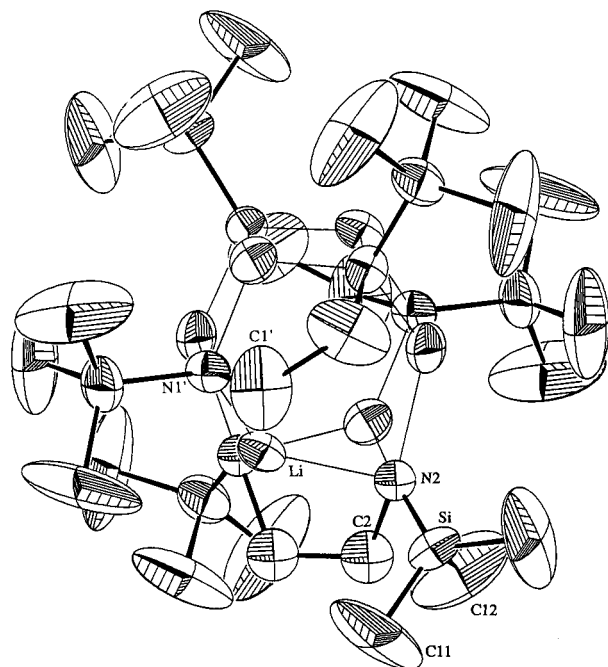
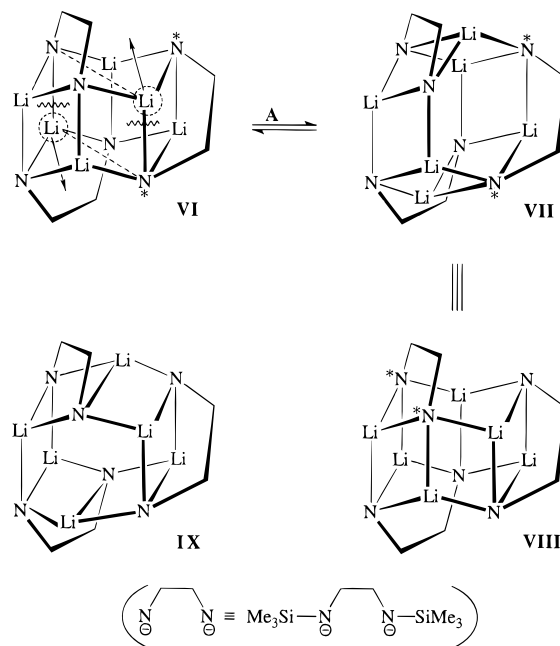


**Figure 4.** Molecular projection of  $[\{Li[N(SiMe_3)CH_2CH_2NSiMe_3-Li\}_3]$ , **3**, showing the atom-labeling scheme. Thermal ellipsoids are drawn at the 20% probability level.

of coalescing at 50 °C. Lowering the temperature reverses the intensity distribution of the two resonances, the relative intensities of the two resonances following that observed in the  $^1H$  NMR spectrum. The two resonances are assigned as belonging to the two species indicated in the  $^1H$  NMR spectrum. At low temperature the dominant resonance broadens to become almost indistinguishable from the baseline at -40 °C and then sharpens slightly below this temperature. In the limit, two broad signals at 1.56 and 0.98 ppm are observed in a *ca.* 4:1 ratio.  $^7Li$  NMR chemical shifts in organolithium complexes devoid of  $\pi$ -complexed aromatic interactions typically cover a narrow range and coupled with the broad line widths at low temperature may be hindering the observation of distinct  $^7Li$  resonances for each inequivalent  $^7Li$  nucleus of the dominant species in the low temperature limit and should not necessarily be taken as evidence for a fast exchange process at this temperature.<sup>14</sup>

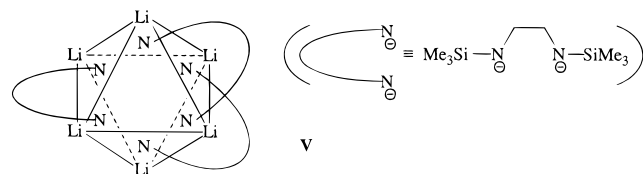
Rationalization of the NMR data for **3** both enables us to make a confident identification of the two species in solution and enables us to postulate the exchange process which gives rise to the observed fluxional behavior for one of the species. The species which at low temperature exhibits three chemically distinguishable trimethylsilyl groups is consistent with the crystal structure of complex **3**. The trimeric structure exhibits  $C_2$  molecular symmetry and as such contains three chemically distinguishable trimethylsilyl groups, six chemically distinguishable methylene protons, and three chemically distinguishable lithium atoms. Considering that a monomer would be unlikely in the absence of donor solvents, the smaller aggregate is likely to be a dimer. The dimer is most likely to exhibit a  $Li_4N_4$  cage formed by the stacking of two dilithium bridged monomers, the same as that proposed for the solution structure of the etherate **2**, *cf.*, the crystal structures of  $[\{Li[rac-N(t-Bu)CH(Me)CH(Me)N(t-Bu)]Li\}_2]^3$  and  $[\{Li[N(t-Bu)Si(Me)_2N(t-Bu)-Li\}_2]$ .<sup>15</sup> Such a dimer contains chemically equivalent trimethylsilyl groups, which is consistent with the low temperature

**Scheme 3**



NMR data for this species. For temperatures in the range -80 to +50 °C there is no evidence for rapid exchange on the NMR time scale between the two species present in solution, indicating that the fluxional process which gives rise to the room temperature equivalence of all six trimethylsilyl groups of the trimer is intramolecular.

The crystal structure of the trimer **3** can be looked on as a distorted octahedral (trigonal antiprismatic) arrangement of six lithium atoms with six of the eight faces of the distorted  $Li_6$  octahedron being associated with triply bridging amido nitrogen atoms, as depicted in **V**, a schematic projection of the trimer viewed in the direction of the two opposite uncapped faces of the distorted octahedron of lithium atoms.



The process which gives rise to the observed dynamic behavior of the trimer probably involves the distortion of the  $Li_6$  core of the molecule, Scheme 3. Movement of two of the opposing lithium atoms (circled in **VI**) with concomitant cleavage and formation of two  $Li-N$  bonds (marked with fractures and dashes, respectively, in **VI**) interconverts the "ladder face-bridging" (asterisked) ligand to a "ladder edge-bridging" ligand shown in **VII**, which is redrawn in **VIII**, equilibrium **A**. Alternatively, this process can be looked on as being a chair-boat interconversion of the two stacked  $Li_3N_3$  rings to give an equivalent structure with the ligands interchanged. The temperature dependence observed for the trimethylsilyl group protons of the trimer is consistent with this process. Moreover, the fluxional process would result in a time averaged structure of the trimer having three equivalent "ladder face-bridging" ligands, **IX**. Such a structure has  $D_3$  molecular symmetry and as such contains six chemically equivalent trimethylsilyl groups, six chemically equivalent lithium atoms, and two chemically distinguishable methylene protons; the NMR resonances would exhibit an  $AA'XX'$  spin system which is consistent with the observed spin system for those protons above -20 °C.

(14) Hoffmann, D.; Dorigo, A.; Schleyer, P. v. R.; Reif, H.; Stalke, D.; Sheldrick, G. M.; Weiss, E.; Geissler, M. *Inorg. Chem.* **1995**, *34*, 262.

(15) Brauer, D. J.; Bürger, H.; Liewald, G. R. *J. Organomet. Chem.* **1986**, *308*, 119.

**X-ray Structure Commentary.** The crystal structure determinations show the compounds are comprised of discrete dimeric, **2**, and trimeric species, **3**, respectively, with both structures being solved by direct method routines. Complex **2** crystallizes as prismatic crystals in the monoclinic space group  $P2_1/n$  (No. 14) with four dimers in the unit cell, the asymmetric unit containing one dimer of composition  $[\{\text{Li}[\text{N}(\text{SiMe}_3)\text{CH}_2\text{CH}_2\text{NSiMe}_3]\text{Li}\cdot\text{OEt}_2\}_2]$ , Figure 3. Disorder in the diethyl ether molecules was apparent in Fourier maps but could not be successfully modelled. Refinement of the disordered diethyl ether molecules by a single conformation with large anisotropic thermal parameters led to a  $R$ -factor of 5.9%. Complex **3** crystallizes as prismatic crystals in the trigonal space group  $R\bar{3}m$  (No. 166) with three trimers in the unit cell, the asymmetric unit containing  $1/12$ th of a benzene molecule and  $1/12$ th of the trimer of composition  $[\{\text{Li}[\text{N}(\text{SiMe}_3)\text{CH}_2\text{CH}_2\text{NSiMe}_3]\text{Li}\}_3]$ , Figure 4. Severely disordered molecules of **3** reside on sites of  $D_{3d}$  symmetry,  $(1/3, 1/3, 5/6)$ . The trimethylsilyl group and the lithium atoms were refined anisotropically with large thermal parameters with a fixed site occupation of 1. One of the two positions of the disordered methylene carbons in a "ladder edge-bridging" position of the cyclic ladder was located along with the associated amido-nitrogen atom and refined anisotropically with a fixed site occupation of  $2/3$ . The remaining methylene carbon position was located in a "ladder face-bridging" position of the cyclic ladder and refined isotropically with a fixed site occupation of  $1/6$ . The amido nitrogen atom associated with the "ladder face-bridging" methylene carbon was located and refined isotropically with a fixed site occupation of  $1/3$ . Connectivity of the ethylene linkages of the ligands in the trimer necessitated the constrained population parameters of the disordered atoms outlined above. The trimethylsilyl group and the lithium atom associated with the lower occupancy methylene carbons could not be located but were absorbed into the thermal motion of the higher occupancy positions of the same atoms, accounting for the high thermal motion of these atoms. This disorder model led to a  $R$ -factor of 12.1%. Refinement of the structure in the related space groups  $R\bar{3}$  (No. 148) and  $R32$  (No. 155) gave higher final residuals. Correlation matrix elements for all three refinements did not favor any one of the space groups, and the refinement which led to the lowest  $R$ -factor is presented.

Complex **2** is best described as a bis(diethyl ether) adduct of an amido-lithium complex containing a four-rung  $\text{Li}_4\text{N}_4$  ladder core. The complex contains three coordinate lithium atoms. The three coordination sites of the two "central" lithium atoms are occupied by three bridging amido nitrogen atoms while the coordination sphere of the two "terminal" lithium atoms contains two bridging amido nitrogen atoms and is complemented by an oxygen atom of the coordinating diethyl ether molecules. The molecule has noncrystallographic  $C_2$  symmetry.

Selected geometrical parameters are given in Table 4. The Li-N(amido) distances in **2** occur in two exclusive ranges. The Li-N distances to the triply bridging, five coordinate amido nitrogens are in the range 2.03(2)–2.14(2) Å while the Li-N distances to the doubly bridging four coordinate amido nitrogens fall within the range 1.91(2)–1.98(2) Å. These groupings are close to those observed in the four-rung ladder structures of  $[\{\text{Li}[\text{N}(t\text{-Bu})\text{CH}_2\text{CH}_2\text{N}(H)(t\text{-Bu})]\}_2\text{Li}\{\text{N}(t\text{-Bu})\text{CH}_2\text{CH}_2\text{N}(t\text{-Bu})\text{-Li}\}]^7$  and  $[\{\text{LiN}(\text{CH}_2)_4\}_6(N,N,N',N'',N'''\text{-pentamethyldiethylenetriamine})_2]$ ,<sup>16</sup> which have Li-N(triply bridging amido) distances of 2.02–2.13 and 2.03–2.14 Å, respectively, and Li-N(doubly bridging amido) distances within the ranges 1.95–2.00 and

1.91–1.98 Å, respectively. Comparisons with the crystal structures of the other four-rung lithium amide ladders  $[\{\text{Li}[\text{N}(\text{CH}_2)_5]\{\text{HN}(\text{CH}_2)_5\}_4]$ ,<sup>17</sup>  $[\{\text{LiN}(\text{CH}_2)_4\}_4(N,N,N',N''\text{-tetramethylethylenediamine})_2]$ ,<sup>18</sup> and  $[\{\text{Li}_2[\text{N}(2,6\text{-}i\text{-Pr}_2\text{C}_6\text{H}_3)\text{CH}_2\text{CH}_2\text{N}]\}_2]$ <sup>19</sup> are less valid given the different coordination numbers of the terminal lithium atoms in those cases.

The Li–O distances in **2**, 1.95(2) Å, are typical for diethyl ether solvates of amidolithium species, comparing with the Li–O distances of 1.943(6) and 1.96(1) Å in the three-coordinate lithium amide dimers  $[\{\text{Et}_2\text{O}\cdot\text{Li}[\mu\text{-N}(\text{SiMe}_3)_2]\}_2]$ <sup>20,21</sup> and  $[\text{trans-}\{\text{Et}_2\text{O}\cdot\text{Li}[\mu\text{-N}(H)\text{B}(2,4,6\text{-Me}_3\text{C}_6\text{H}_2)]_2\}_2]$ .<sup>22</sup> The Li–O distance in the substituted amidolithium dimer  $[\text{trans-}\{\text{Et}_2\text{O}\cdot\text{Li}[\mu\text{-NH}(2,4,6\text{-}t\text{-Bu}_3\text{C}_6\text{H}_2)]_2\}_2]$ ,<sup>23</sup> is significantly shorter at 1.906(5) Å, while still having three-coordinate lithium atoms.

Close Li···Li contacts are observed across each of the  $\text{Li}_2\text{N}_2$  rings of **2**, the distances in the end  $\text{Li}_2\text{N}_2$  rings, 2.40(2) Å, being marginally longer than in the central  $\text{Li}_2\text{N}_2$  ring, 2.31(2) Å. Each of the central lithium atoms exhibit two close Li–H contacts with the calculated methyl protons of the one methyl group in the range 2.43–2.46 Å. These contacts are some 0.2 Å longer than those observed for the protons of lithium amides derived from *N*-*tert*-butyl-substituted ethylenediamines<sup>3,7</sup> but are still 0.6 Å less than the sum of the van der Waals radii of the lithium and hydrogen atoms.

The coordination environments of the lithium atoms in **2** differ considerably. The sum of the three N–Li–N angles about the central lithium atoms are 318.3 and 319.7°, indicative of a pyramidal coordination environment which leaves a large portion of the coordination sphere of the lithium atoms devoid of primary interactions. Steric hindrance to each of these lithium atoms is afforded by three trimethylsilyl substituents blocking coordination of the lithium atoms by diethyl ether, which would almost certainly disrupt the ladder structure, *viz.*, theoretical calculations on solvated  $\text{LiNH}_2$  aggregates.<sup>1</sup> The terminal lithium atoms in comparison have nearly planar coordination environments,  $\sum(\text{N},\text{O}-\text{Li}-\text{N}) = 359.7$  and  $359.9^\circ$ , owing to the freedom of diethyl ether to position itself according to VSEPR theory and not being constrained by ligand bite angles, *etc.*, as in the case of the amido nitrogens.

The three  $\text{Li}_2\text{N}_2$  rings in the four-rung ladder of **2** are folded only slightly. The end  $\text{Li}_2\text{N}_2$  rings are nearly flat, again owing to the freedom of the Li–OEt<sub>2</sub> fragment to position itself without ligand geometry constraints the Li–N–N–Li dihedral angles measure 171(1) and 173(1)°. The central  $\text{Li}_2\text{N}_2$  ring is somewhat more folded, the Li–N–N–Li dihedral angle measuring 157(1)°. The largest deviation of the four-rung  $\text{Li}_4\text{N}_4$  ladder from planarity results from the "edge-bridging" ethylene linkages of the dilithiated ethylenediamines, which pull the ladder around into a highly "concave" or "U-shaped" conformation. This concavity is measurable as the dihedral angles between the planes of the terminal and central  $\text{Li}_2\text{N}_2$  rings. The observed dihedral angles of 59.1(7) and 57.6(7)° contrast with

(16) Armstrong, D. R.; Barr, D.; Clegg, W.; Mulvey, R. E.; Reed, D.; Snaith, R.; Wade, K. *J. Chem. Soc., Chem. Commun.* **1986**, 869.

(17) Boche, G.; Langlotz, I.; Marsch, M.; Harms, K.; Nudelman, N. E. S. *Angew. Chem.* **1992**, *104*, 1239; *Angew. Chem., Int. Ed. Engl.* **1992**, *31*, 1205.

(18) Armstrong, D. R.; Barr, D.; Clegg, W.; Hodgson, S. M.; Mulvey, R. E.; Reed, D.; Snaith, R.; Wright, D. S. *J. Am. Chem. Soc.* **1989**, *111*, 4719.

(19) Chen, H.; Bartlett, R. A.; Dias, H. V. R.; Olmstead, M. M.; Power, P. P. *Inorg. Chem.* **1991**, *30*, 2487.

(20) Lappert, M. F.; Slade, M. J.; Singh, A.; Atwood, J. L.; Rogers, R. D.; Shakir, R. *J. Am. Chem. Soc.* **1983**, *105*, 302.

(21) Engelhardt, L. M.; May, A. S.; Raston, C. L.; White, A. H. *J. Chem. Soc., Dalton Trans.* **1983**, 1671.

(22) Bartlett, R. A.; Chen, H.; Dias, H. V. R.; Olmstead, M. M.; Power, P. P. *J. Am. Chem. Soc.* **1988**, *110*, 446.

(23) Cetinkaya, B.; Hitchcock, P. B.; Lappert, M. F.; Misra, M. C.; Thorne, A. J. *J. Chem. Soc., Chem. Commun.* **1984**, 148.

the dihedral angle of  $0^\circ$  expected for a flat ladder. The edge-bridging ethylene linkages of **2** can be viewed as being remnants of the stacked dimer of  $[\{\text{Li}[\text{N}(\text{SiMe}_3)\text{CH}_2\text{CH}_2\text{NSiMe}_3]\text{Li}\}_2]$  which has been capped on two corners of the  $\text{Li}_4\text{N}_4$  cage by two molecules of diethyl ether, resulting in cleavage of two edges of the cage, giving the observed ladder structure of **2**, *vide supra*. The ladder structure of  $[\{\text{Li}_2[\text{N}(2,6\text{-}i\text{-Pr}_2\text{C}_6\text{H}_3)\text{CH}_2\text{CH}_2\text{N}\}_2]$ <sup>19</sup> is also contorted owing to the ethylene linkages of the dilithiated ethylenediamines "edge-bridging" the nitrogen atoms along the ladder. However the ladder is centrosymmetric, and the effect is to form a step in the ladder. The dihedral angle between the planes of the terminal and central  $\text{Li}_2\text{N}_2$  rings is greater in that case, measuring  $72.5^\circ$ .

The N(amido)–Si distances in **2**, 1.678(7)–1.709(8) Å, are contracted relative to typical nonmetalated silylamines which is consistent with the stabilization of charge onto the polarizing silyl substituents.<sup>24</sup> The extent of contraction observed for **2** is similar to that found in  $[\{\text{Li}[\text{N}(t\text{-Bu})\text{CH}_2\text{CH}_2\text{N}(\text{H})(t\text{-Bu})]\}_2\text{Li}\{\text{N}(\text{SiMe}_3)\text{CH}_2\text{CH}_2\text{NSiMe}_3\}\text{Li}]$ ,<sup>7</sup> 1.711(4)–1.714(4) Å. Other bond angles within the molecule are unexceptional and do not require comment.

Owing to the severe disorder in the crystal structure of **3**, structural commentary will largely be restricted to qualitative aspects. Selected geometrical parameters are given in Table 5. The trimer consists of a trigonal antiprismatic, or distorted octahedral arrangement of six lithium atoms containing six short, 2.27(4)–2.32(4) Å, and six long  $\text{Li}\cdots\text{Li}$  contact distances, 3.06 Å, analogous to the known hexamers in alkyl- and imidolithium chemistry, for example,  $[(c\text{-HexLi})_6]$ <sup>25</sup> and  $[\{\text{LiN}=\text{C}(\text{Ph})(t\text{-Bu})\}_6]$ ,<sup>11</sup> and the crystal structure of  $[\{\text{LiN}(\text{CH}_2)_6\}_6]$ .<sup>26</sup> Six

faces of the octahedron are each capped by a  $\text{NR}_2$  unit and the two equilateral (and opposite) faces with the longest triangular side lengths unoccupied. The triangular faces capped by the amido nitrogen atoms are isosceles in shape. Five of the six  $\text{Li}_2\text{N}_2$  rings of the cyclized ladder are essentially planar. The  $\text{Li}_2\text{N}_2$  ring defined by the ladder "face-bridging" ethylenediamido ligand is folded along the N–N vector, the dihedral angle measuring  $131^\circ$ , similar to the dihedral angles found for the folded  $\text{Li}_2\text{N}_2$  rings in  $[\{\text{Li}[\text{rac-N}(t\text{-Bu})\text{CH}(\text{Me})\text{CH}(\text{Me})\text{N}(t\text{-Bu})]\text{Li}\}_2]$ <sup>3</sup> and  $[\{\text{Li}[\text{N}(t\text{-Bu})\text{CH}_2\text{CH}_2\text{N}(\text{H})(t\text{-Bu})]\}_2\text{Li}\{\text{N}(t\text{-Bu})\text{CH}_2\text{CH}_2\text{N}(t\text{-Bu})\}\text{Li}]$ ,<sup>7</sup> 123(1) and  $110.1(6)^\circ$ , respectively. The  $\text{Li}_4\text{N}_4$  ladder section of the cyclic trimer **3** common to the dimeric etherate **2** remains essentially unaltered; the dihedral angles between adjacent  $\text{Li}_2\text{N}_2$  rings in **2**, 59.1(7) and  $57.6(7)^\circ$ , are close to those in **3**, crystallographically constrained to be  $60^\circ$ . Following directly from this, the transannular  $\text{Li}\cdots\text{N}$  contacts across the  $\text{Li}_3\text{N}_3$  rings in **3**, 3.56 Å, are slightly reduced relative to the analogous contacts in **2**, 4.00 and 4.02 Å, having been affected by the completion of the  $\text{Li}_6\text{N}_6$  cyclic ladder in **3** vs diethyl ether coordination of the terminal lithium atoms in **2**. Other bond angles within the molecule are unexceptional and do not require comment.

**Acknowledgment.** We gratefully acknowledge support of this work by the Australian Research Council, and we thank Colin Kennard and Karl Byriel for collecting the X-ray diffraction data.

**Supporting Information Available:** Lists of  $U_{ij}$  values, hydrogen atom parameters, bond distances and angles, and summaries of the X-ray diffraction data (7 pages) for compounds **2** and **3**. Ordering information is given on any current masthead page.

IC9510425

(24) (a) Dippel, K.; Klingebiel, U.; Noltemeyer, M.; Pauer, F.; Sheldrick, G. M. *Angew. Chem.* **1988**, *100*, 1093; *Angew. Chem., Int. Ed. Engl.* **1988**, *27*, 1074. (b) Glidewell, C.; Thomson, C. *J. Comput. Chem.* **1982**, *3*, 495.

(25) Zenger, R.; Rhine, W.; Stucky, G. D. *J. Am. Chem. Soc.* **1974**, *96*, 6048.

(26) Barr, D.; Clegg, W.; Hodgson, S. M.; Lamming, G. R.; Mulvey, R. E.; Scott, A. J.; Snaith, R.; Wright, D. S. *Angew. Chem.* **1989**, *101*, 1279; *Angew. Chem., Int. Ed. Engl.* **1989**, *28*, 1241.